

2

3 **Pion femtoscopy in p/d+Au collisions at**
4 **$\sqrt{s_{NN}} = 200$ GeV in the STAR experiment**

5 *E. Khyzhniak* ^{a,1} (for the STAR Collaboration)

6 ^a National Research Nuclear University MEPhI, Kashirskoe highway 31, Moscow, 115409,
Russia

7 It is interesting to see how the space-time characteristics of the region of particle emission created during nuclear collisions change as the colliding nuclei get bigger. At an energy of 200 GeV per nucleon pair, the STAR experiment allows one to investigate the properties of the created medium for two colliding systems with nearly identical sizes: p+Au and d+Au. As a result, the difference in particle emission region properties introduced by just one more nucleon may be detected. Using the femtoscopy technique it becomes possible to perform this measurement.

The paper investigates the dependence of the emission region's invariant radii on the transverse momentum of pion pairs for various multiplicities in the p+Au and d+Au collision systems. The physical implication is also presented in this paper.

8 Интересно посмотреть как пространственно-временные характеристики области испускания частиц, создающейся во время столкновения, меняются с увеличением размером начальной системы столкновения. При энергии 200 ГэВ на пару нуклонов, эксперимент STAR позволяет исследовать свойства возникающей среды после соударения двух систем с близкими размерами: p+Au и d+Au. В результате, можно обнаружить разницу свойств области испускания частиц для систем отличающихся всего на один нуклон. Это измерение возможно выполнить с помощью техники корреляционной фемтоскопии.

9 В этой статье исследуется зависимость инвариантного радиуса области испускания частиц от поперечного импульса пар пионов для различных диапазонов по множественности в столкновениях p+Au и d+Au при $\sqrt{s_{NN}} = 200$ GeV. Физическая составляющая обсуждается.

10 1. Introduction

11 The correlation femtoscopy technique can be used to measure the spatial and temporal extents of the emission region in high-energy heavy-ion collisions. These correlations are influenced by quantum statistics, Coulomb interactions, and strong final state interactions. The collision dynamics [1] essentially define the spatio-temporal structure of the particle-emitting source. The system expansion dynamics are influenced by the medium's transport properties, the phase transition/critical point, and the event shape.

12 Examining the spatial and temporal scales of the particle-emitting source is one method for studying the particle production process. Small colliding systems (such as

¹E-mail: eugenia.sh.el@gmail.com

19 p+Au or d+Au) are sensitive to initial conditions. As a result, the precise nature of
 20 particle production becomes critical [2, 3].

21 This paper presents the invariant radii of charged pions obtained for p+Au and d+Au
 22 collisions at $\sqrt{s_{NN}} = 200$ GeV recorded in the STAR experiment. The pion-pair trans-
 23 verse momentum dependence of the source radii reflects the system's collective expansion
 24 and allows one to investigate different regions of homogeneity in both p+Au and d+Au
 25 systems. The dependence of invariant radii on pair transverse momentum and charged
 26 particle multiplicity is discussed.

27 2. Femtoscopy

28 The femtoscopy technique is used to measure the space-time extents of the particle-
 29 emitting area at kinetic freeze-out of collisions. The quantum statistical correlations
 30 between two identical particles [4–7] lies beneath this technique as a foundation. Usually,
 31 for the 1D case, the femtoscopic correlations are studied as a function of pairs' relative
 32 momentum, $Q_{inv} = \sqrt{(\mathbf{p}_1 - \mathbf{p}_2)^2 - (E_1 - E_2)^2}$, where \mathbf{p}_1 , \mathbf{p}_2 are particle 3-momenta
 33 and E_1 , E_2 are particle energies.

34 Experimental correlation function is defined as follows::

$$35 \quad C(Q_{inv}) = \frac{A(Q_{inv})}{B(Q_{inv})}, \quad (1)$$

36 in this equation $A(Q_{inv})$ is a pairs' relative momentum distribution which incorporates
 37 the Bose-Einstein statistics, Coulomb, and strong interactions, whereas $B(Q_{inv})$ is a
 38 reference distribution which includes all experimental effects except for physical correla-
 39 tions between particles. To remove the physical correlations between particles but keep
 40 acceptance effects as in $A(Q_{inv})$, an event mixing technique [8] was used to reconstruct
 41 $B(Q_{inv})$ in this work.

42 For the next step, to extract the actual parameters from the correlation function, we
 43 do fit $C(Q_{inv})$ with the following function [9, 10]:

$$44 \quad C(Q_{inv}) = N(1 - \lambda + \lambda K_{Coul}(Q_{inv})(1 + G(Q_{inv})))D(Q_{inv}), \quad (2)$$

45 where N is a normalization factor, λ is a correlation strength parameter, $D(Q_{inv})$ is a non-
 46 femtoscopic contribution (in this work it is $D(Q_{inv}) = 1$), $K_{Coul}(Q_{inv})$ is a squared like-
 47 sign pion pairs' Coulomb wave-function integrated over the spherical Gaussian source [11,
 48 12], and $G(Q_{inv}) = e^{-Q_{inv}^2 R_{inv}^2}$ is the Gaussian form of the emission source, where R_{inv}
 49 is an estimation of the emission source's size. It is also possible to study dynamics of
 50 the system evolution by measuring the pairs' transverse momentum, $k_T = \frac{|\mathbf{p}_{1T} + \mathbf{p}_{2T}|}{2}$,
 51 dependence of the correlation function [13].

3. Analysis details

This study makes use of data from p+Au and d+Au collisions at $\sqrt{s_{NN}} = 200$ GeV collected by the STAR experiment. The event was chosen for investigation if the z-position of the collision vertex was within 40 cm from the center of the Time Projection Chamber (TPC) [14]. At the same time, the radial component of the collision vertex point must not exceed 2 cm relative to the beam center. There could be pile-up events, i.e. several collisions occur in the collider during the readout of the event in the TPC's gas volume. To obtain an independent estimate of the position of the collision point in STAR, two VPD [15] detectors are located ~ 5.7 m from the center of TPC along the beam axis. To remove the pile-up, events with a difference in the z-positions of the primary vertex obtained from TPC and VPD greater than 5 cm in absolute value were excluded from the analysis. Particle tracks were selected from momentum range $p \in [0.15, 0.8]$ GeV/c, and from pseudorapidity range $|\eta| < 0.5$. The particles were identified using ionization energy losses of charged particles in TPC's sensitive volume. Only tracks with splitting level (SL) [16], $-0.5 < SL < 0.6$, average separation of two tracks from the pair within TPC volume > 10 cm, and fraction of merged hits (FMR), $FMR \in [-1.1, 0.1]$ were utilized in the study to exclude two-track effects such as track-merging and track-splitting. The splitting level value indicates if a pair's two tracks are indeed two tracks or if one track has been reconstructed as two tracks with similar momenta. When two particles are reconstructed as one track, the situation can be reversed. The FMR [16] was used to estimate the impact of this effect.

It is crucial to consider the extent of the systematic error, as it may turn out to be more significant than the statistical errors. The range of fit (Q_{inv}) and the size of the Coulomb radius, as well as the criteria for selecting events, tracks, and pairs of pions, were all considered as causes of systematic errors. The cuts on the primary vertex's position (which had a 5% effect on the values of invariant radii), the momentum of the selected tracks and tracking efficiencies ($>6\%$), and the criteria of merging and splitting ($>2\%$) were all varied within reasonable ranges. The fit range was also varied to account for the accuracy of determining the minimum of χ^2 in the fit; the influence on the final radii was less than 3%. The radius of the Coulomb interaction was also varied, however the effect on the correlation function was quite small, only about 3%.

Total systematic uncertainty was calculated as a quadratic sum of the differences between individual and average ones.

4. Results

Figure 1 illustrates an example of correlation functions measured for identical charged pion pairs from d+Au and p+Au collisions at $\sqrt{s_{NN}} = 200$ GeV for the multiplicity range $11 < N_{ch}^{|\eta| < 0.5} < 20$ and transverse momentum range $k_T \in [0.25, 0.35]$ GeV/c. Also, Fig. 1(a) shows the fit to the correlation functions with Eq. (2), where $G(Q_{inv}) = e^{-Q_{inv}^2 R_{inv}^2}$ has a Gaussian form, whilst Fig. 1(b) shows the fit to the correlation functions with the same Eq. (2), but the $G(Q_{inv}) = e^{-Q_{inv} R_{inv}}$ has an exponential form. They are tested to check if the emitting source follows Lorentzian or Gaussian distributions.

93 The fit of the correlation functions by Eq. (2) is represented by the red and blue lines.
 94 The correlation functions are reasonably described by the fits. The Gaussian assumption
 95 was used for all subsequent results, since the regions of homogeneity are defined only for
 96 the assumption of Gaussian parametrization [13].

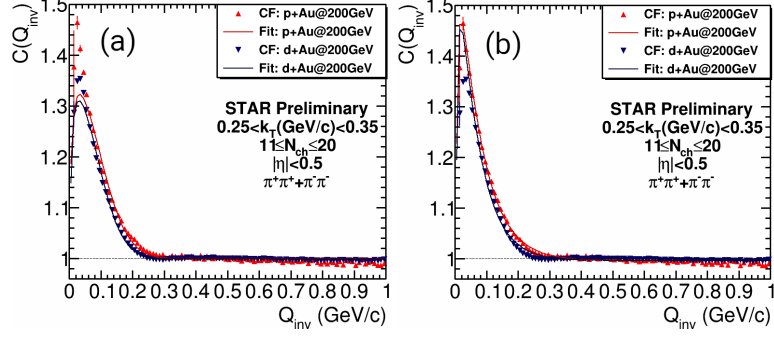


Figure 1. (Color online) Example of the Gaussian (a) and Exponential (b) assumption of fit to the identical pion pairs correlation functions for d+Au (blue) and p+Au (red) collisions at $\sqrt{s_{NN}} = 200$ GeV for the multiplicity range $11 < N_{ch}^{|\eta| < 0.5} < 20$ and transverse momentum range $k_T \in [0.25, 0.35]$ GeV/c.

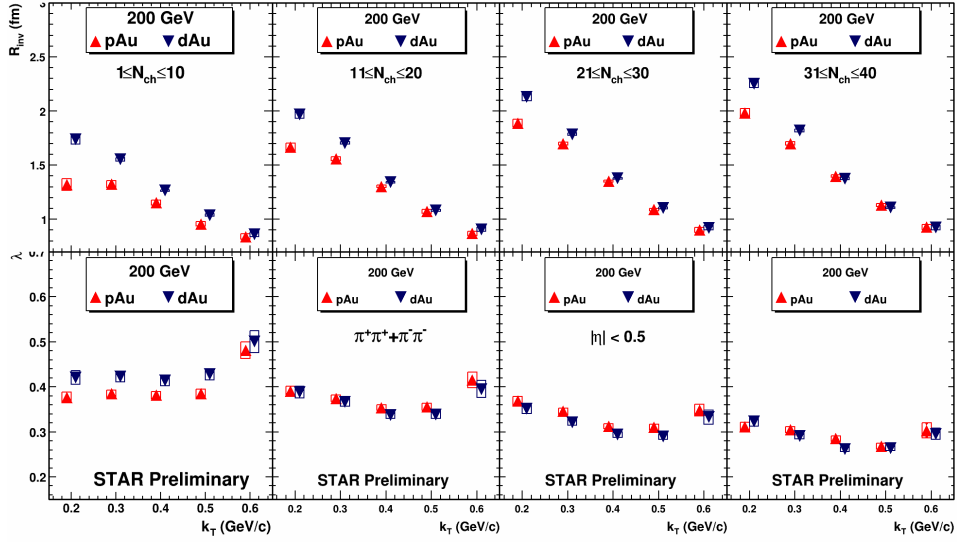


Figure 2. (Color online) Dependences of identical charged pion invariant radii (top row) and correlation strength parameter (bottom row) on k_T and multiplicity for p+Au and d+Au collisions at $\sqrt{s_{NN}} = 200$ GeV. Statistical and systematic uncertainties are shown by vertical lines and boxes, respectively. In almost all cases, statistical uncertainties are smaller than the marker size.

97 To investigate the space-time structure of the pion emission source in p+Au and
 98 d+Au collision systems at $\sqrt{s_{NN}} = 200$ GeV, the dependence of the invariant radii on
 99 the transverse momentum of the pairs is shown. Figure 2 shows that the invariant radii
 100 have a falling dependence on k_T , indicating the presence of collective radial flow in small
 101 collision systems. Figure 2 also demonstrates the radius dependence on the particle
 102 multiplicity created in the collisions. The radii increase as the multiplicity increases,
 103 which is to be expected given the geometric form of collisions. The increase of invariant
 104 radii with increasing colliding system size, while the difference between the radii of the
 105 two systems decreases significantly with increasing transverse momentum of pion pairs
 106 and the multiplicity of particles formed in the collision, is also an interesting observation
 107 from this figure.

108 5. Conclusions

109 The invariant radii of identical charged pions for p+Au and d+Au collisions at
 110 $\sqrt{s_{NN}} = 200$ GeV have been reported and explored in terms of pair transverse mo-
 111 mentum and multiplicity. The radii were found to increase as the multiplicity increases.
 112 This research also demonstrates that the charged pion R_{inv} has a weak dependence on
 113 colliding systems, and that the difference between two colliding systems decreases as the
 114 pair transverse momentum increases. The invariant radii become larger as the colliding
 115 system increases in size.

116 Acknowledgments

117 The work was supported by the Ministry of Science and Higher Education of the Rus-
 118 sian Federation, Project ‘‘Fundamental properties of elementary particles and cosmology’’
 119 No 0723-2020-0041.

120 References

- 121 1. *Pratt S.* Pion interferometry of quark-gluon plasma // Phys. Rev. D. 1986. V. 33. P.
122 1314-1327.
- 123 2. *Bzdak A., Schenke B., Tribedy P., Venugopalan R.* Initial state geometry and the role
124 of hydrodynamics in proton-proton, proton-nucleus and deuteron-nucleus collisions
125 // Phys. Rev. C. 2013. V. 87. P. 10.
- 126 3. *Plumberg C.* Hanbury Brown–Twiss Interferometry and Collectivity in Small Systems
127 // arXiv:2008.01709
- 128 4. *Goldhaber G., Fowler W. B., Goldhaber S., Hoang T.F.* Pion-pion correlations in
129 antiproton annihilation events // Phys. Rev. Lett. 1959. V. 3. P. 181-183.
- 130 5. *Goldhaber G., Goldhaber S., Lee W.-Y., Pais A.* Influence of Bose-Einstein statistics
131 on the anti-proton proton annihilation process // Phys. Rev. 1960. V. 120. P. 300-312.

- 132 6. *Kopylov G.I., Podgoretsky M.I.* Correlations of identical particles emitted by highly
133 excited nuclei // *Sov. J. Nucl. Phys.* 1972. V. 15. P. 219-223.
- 134 7. *Kopylov G.I., Podgoretsky M.I.* Multiple production and interference of particles
135 emitted by moving sources // *Sov. J. Nucl. Phys.* 1974. V. 18. P. 336-341.
- 136 8. *Kopylov G.I.* Like particle correlations as a tool to study the multiple production
137 mechanism // *Phys. Lett. B.* 1974. V. 50. P. 472-474.
- 138 9. *Bowler M.G.* Coulomb corrections to Bose-Einstein correlations have been greatly
139 exaggerated // *Phys. Lett. B.* 1991. V. 270. P. 69-74.
- 140 10. *Sinyukov Yu., Lednicky R., Akkelin S.V., Pluta J., Erasmus B.* Coulomb corrections
141 for interferometry analysis of expanding hadron systems // *Phys. Lett. B.* 1998. V.
142 432. P. 248-257.
- 143 11. *Bowler M.G.* Coulomb corrections to Bose-Einstein correlations have been greatly
144 exaggerated // *Phys. Lett. B.* 1998. V. 270. P. 69-74.
- 145 12. *Sinyukov Yu., Lednicky R., Akkelin S.V., Pluta J., Erasmus B.* Coulomb corrections
146 for interferometry analysis of expanding hadron systems // *Phys. Lett. B.* 1998. V.
147 432. P. 248-257.
- 148 13. *Akkelin S.V., Sinyukov Yu.M.* The HBT-interferometry of expanding sources //
149 *Phys. Lett. B.* 1995. V. 356. P. 525-530.
- 150 14. *Anderson M. et al.* The Star time projection chamber: A Unique tool for studying
151 high multiplicity events at RHIC // *Nucl. Instrum. Meth. A.* 2003. V. 499. P. 659-678.
- 152 15. *Llope W.J. et al* The STAR Vertex Position Detector // *Nucl. Instrum. Meth. A.*
153 2014. V. 759. P. 23-28.
- 154 16. *Adams J. et al. (STAR Collaboration)* Pion interferometry in Au+Au collisions at
155 $\sqrt{s_{NN}} = 200$ GeV // *Phys. Rev. C.* 2005. V. 71. P 25.